Molecular dynamics simulations for the prediction of thermal conductivity of bulk silicon and silicon nanowires: Influence of interatomic potentials and boundary conditions

Carolina Abs da Cruz, Konstantinos Termentzidis, Patrice Chantrenne, xavier Kleber

Molecular dynamics simulations for the prediction of thermal conductivity of bulk silicon and silicon nanowires: Influence of interatomic potentials and boundary conditions

Carolina Abs da Cruz,[1,2,a)] Konstantinos Termentzidis,[1,2] Patrice Chantrenne,[1,2] and Xavier Kleber[2,3]
[1]*INSA de Lyon, CETHIL UMR5008, F-69621 Villeurbanne, France*
[2]*INSA de Lyon, Université de Lyon, F-69621 Villeurbanne, France and Université Lyon 1, F-69621 Villeurbanne, France*
[3]*INSA de Lyon, MATEIS UMR5510, F-69621 Villeurbanne, France*

(Received 19 April 2010; accepted 1 June 2011; published online 8 August 2011)

The reliability of molecular dynamics (MD) results depends strongly on the choice of interatomic potentials and simulation conditions. Five interatomic potentials have been evaluated for heat transfer MD simulations of silicon, based on the description of the harmonic (dispersion curves) and anharmonic (linear thermal expansion) properties. The best interatomic potential is the second nearest-neighbor modified embedded atom method potential followed by the Stillinger-Weber, and then the Tersoff III. However, the prediction of the bulk silicon thermal conductivity leads to the conclusion that the Tersoff III potential gives the best results for isotopically pure silicon at high temperatures. The thermal conductivity of silicon nanowires as a function of cross-section and length is calculated, and the influence of the boundary conditions is studied for those five potentials. © *2011 American Institute of Physics*. [doi:10.1063/1.3615826]

I. INTRODUCTION

The development of nanotechnology fabrications has led to rising interest in the thermal properties of nanostructures and nanostructured materials. These structures and materials will be included in new microelectronic devices[1,2] and microelectromechanical systems (MEMS)[3,4] whose behavior and reliability strongly depend on the way heat dissipated within the system can be evacuated. Excessive temperatures and temperature gradients may lead to system failure. Thermal conductivity measurements at nanometric scales are not common. Thus, simulation and prediction tools are necessary. Prediction of heat transfer in such systems is a challenge when the thickness of the layers is of the same order of magnitude as the mean free path of heat carriers in the material. Molecular dynamics (MD) is a common and a convenient tool for studying matter at atomic scale. For heat transfer studies, MD is well-suited for dielectric materials since only phonons carry heat.

The literature includes many reviews on silicon potential[5–7] and this abundance of potentials makes it difficult to choose specific theoretical guidance. The choice of potential depends on the type of atomic structure[8] and on the properties to be studied (structural, thermal, etc.).[9] For silicon, the Stillinger-Weber (SW) potential[10] is the most widely used to study heat transfer with MD simulations. It has seven parameters in which the total energy of an atomic configuration is due to a linear combination of two- and three-body terms. Another popular potential is the Tersoff potential. The original version[11] has six adjustable parameters. Two other versions, Tersoff II and Tersoff III, include seven or more parameters to improve elastic properties.[12,13] Two potentials developed by Justo *et al.* (environment-dependent interatomic potential: EDIP)[14] and Lenosky *et al.* (highly optimized empirical potential: HOEP)[15] give partial improvements, but the surface and cluster description properties are less satisfactory than those of the SW and Tersoff potentials.[6] The Bolding-Andersen (BA) potential[16] generalizes the Tersoff potential by using more than 30 adjustable parameters. It describes certain properties correctly (bulk phases, defects, surfaces, and small clusters), but its complexity makes it difficult to perform physical interpretations of its equations.[17] The modified embedded atom method (MEAM) potentials include directional bonding and can be applied to covalent systems. The first nearest-neighbor modified embedded atom method (1NN MEAM) potential was provided by Baskes *et al.*[18] This latter potential was modified by Lee and Baskes[19] to create the second nearest-neighbor modified embedded atom method (2NN MEAM) potential, in order to take into consideration the second nearest-neighbor interactions.

Non-equilibrium molecular dynamics (NEMD) is used to predict the thermal conductivity of nanostructures.[14,20–25] The validity of results depends on the choice of the interatomic potential. To the best of our knowledge, no systematic comparison of potentials for MD heat transfer studies has been reported for silicon. In this article, five potentials are considered to compare their performance for heat transfer studies: SW, Tersoff II, Tersoff III, 1NN MEAM, and 2NN MEAM. These potentials are implemented in a large-scale atomic/molecular massively parallel simulator (LAMMPS).[26] Among the five interatomic potentials under study, three of them were selected in order to predict the thermal conductivity of bulk silicon at 500, 700, and 950 K. The simulation conditions also influence the thermal conductivity of nanostructures[27] and

a)Electronic mail: carolina.abs-da-cruz@insa-lyon.fr.

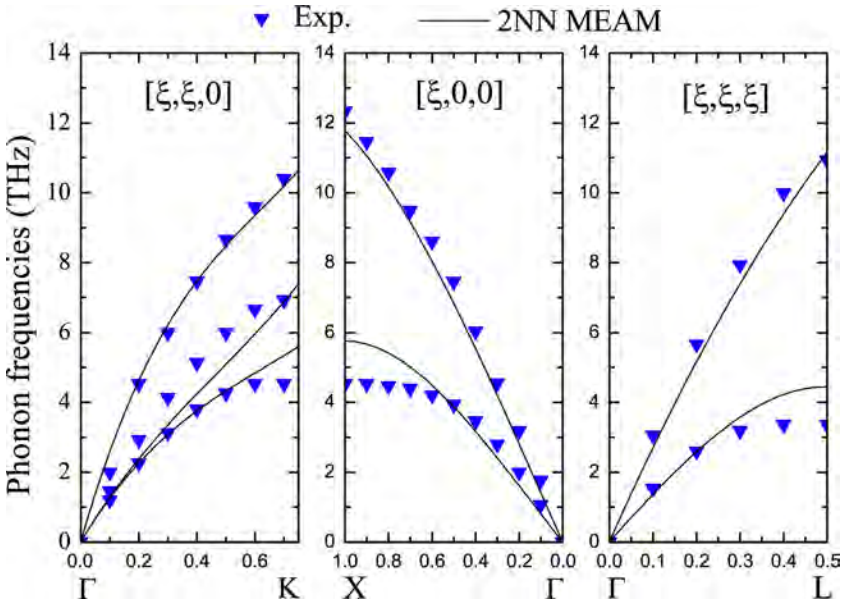

FIG. 1. (Color online) Phonon dispersion curves using the 2NN MEAM potential for bulk silicon (experimental, see Ref. 31).

simulation costs. The influence of the boundary conditions on the thermal conductivity of silicon nanowires is also presented for the five potentials function of the length and the cross-section width of the nanowires.

II. POTENTIALS EVALUATION FOR SILICON

In dielectric materials, heat transfer depends on phonon propagation and interactions. Thus, it is essential to predict dispersion curves in order to choose the most suitable potential for calculating the thermal conductivity. Phonon interactions in a crystalline lattice are due to the anharmonic nature of the interactions. Since thermal expansion is an anharmonic effect, the validity of the interatomic potentials can be determined through the variation of the linear expansion with the temperature. The potentials that can be used for silicon available in LAMMPS[26] are discussed here: SW,[10] Tersoff II,[12] Tersoff III,[13] 1NN MEAM,[18] and 2NN MEAM[6] potentials.

The dispersion curves for bulk Si were determined for the five potentials and then compared to experimental results (Figs. 1, 2, and 3). For the SW, Tersoff II, Tersoff III, and 1NN MEAM potentials, the results for dispersion curves are identical to those previously published.[12,28,29] Dispersion curves for the 2NN MEAM potential are new results. The dispersion relation is calculated from the velocity-velocity autocorrelation function as described by Papanicolaou.[30] To determine the acoustic dispersion curves for bulk materials, periodic boundary conditions are used in all directions. The size of the system in three directions is 10 lattice parameters. Room temperature was chosen for this simulation. Initially, the system was equilibrated for 200 000 time steps after which the simulations were run for 200 000 time steps, with a time step equal to 3 fs in an NVE calculation. The dispersion curves in the [ξ,0,0], [ξ,ξ,0], and [ξ,ξ,ξ] directions were compared with the experimental dispersion curves for Si.[31]

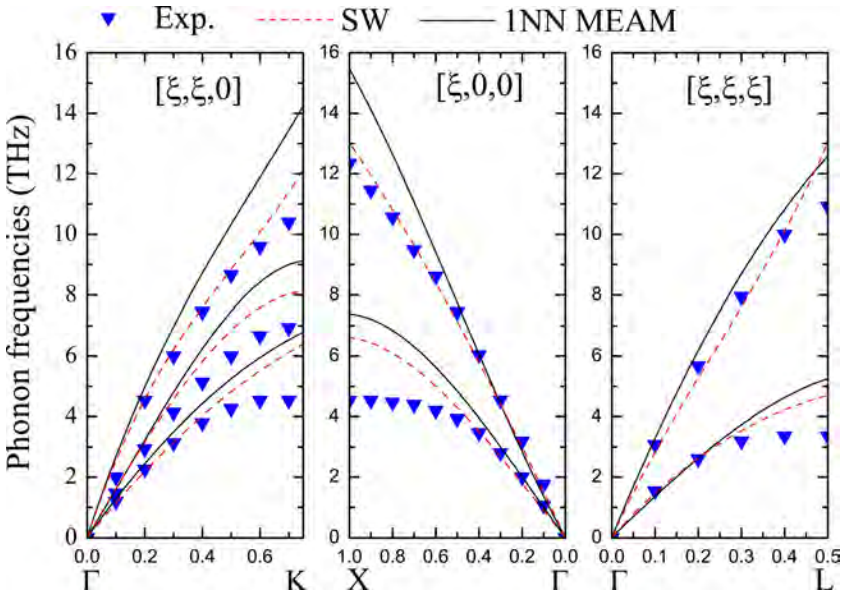

FIG. 2. (Color online) Phonon dispersion curves using the SW and 1NN MEAM potentials for bulk silicon (experimental, see Ref. 31).

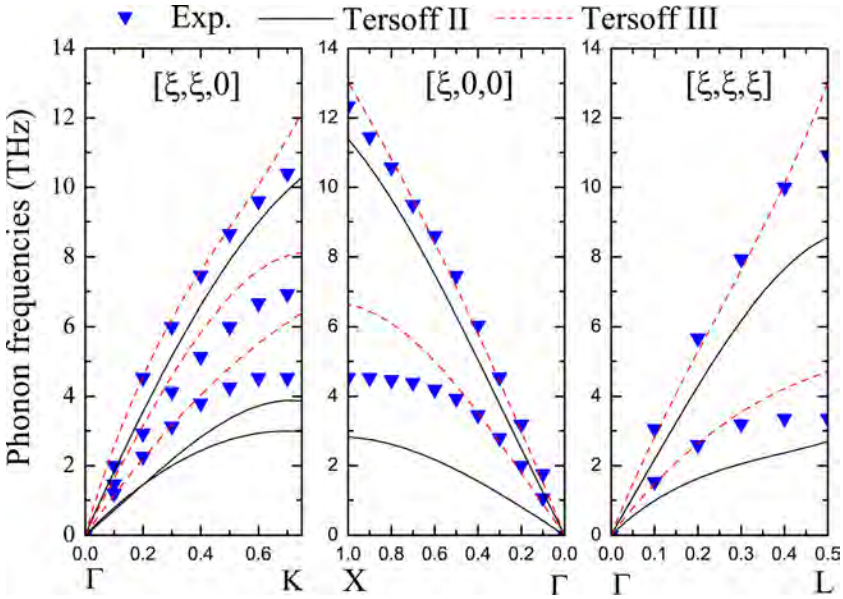

FIG. 3. (Color online) Phonon dispersion curves using the Tersoff II and Tersoff III potentials for bulk silicon (experimental, see Ref. 31).

The optical vibration modes for Si have a much lower group velocity than the acoustic modes, and at low temperatures their energies are also lower than those of acoustic phonons. The contribution of optical vibration modes to thermal conductivity is negligible toward acoustic modes.[32] Therefore, the evaluation of the potential does not consider the quality of the optical modes. However, it is known that acoustic mode diffusion by optical modes is important for reproducing the phonon-phonon relaxation time.[33] Thus, although the quality of optical modes has almost no influence on heat transfer simulations, they are important in relation to the phonon diffusion process that must be reproduced correctly. This criterion is related to the anharmonicity of the potential, evaluated by using the thermal expansion coefficient.

The Tersoff II and 1NN MEAM potentials should not be used for MD heat transfer studies since they do not allow the reproduction of the vibrational and anharmonic behavior of the lattice. Not only does the 1NN MEAM potential greatly overestimate longitudinal and transverse modes,[28] it also greatly overestimates linear thermal expansion.[6,34] On the contrary, Tersoff II underestimates acoustic and longitudinal modes[29] and it also underestimates linear thermal expansion.[7] In addition, Tersoff II gives a negative linear thermal expansion between 300 and 500 K.

SW and Tersoff III overestimate transverse acoustic modes by more than 40% for all large wave vectors,[29] a factor that leads to an increase in thermal conductivity. However, the SW potential is in excellent agreement with the experimental results for linear thermal expansion. Broido *et al.*[35] also used SW and Tersoff potentials in implementing the exact iterative solution of the inelastic phonon Boltzmann equation to compare bulk thermal conductivity. Thermal conductivities are strongly overestimated for temperatures between 100 and 300 K. Broido *et al.*[35] used harmonic and anharmonic criteria to explain the discordant values of thermal conductivity for these potentials and showed that none of these potentials provides satisfactory agreement with experimental results. The 2NN MEAM potential overestimates the transverse acoustic modes by 20% for all large wave vectors. Tersoff III overestimates linear thermal expansion. The SW potential agrees quite well with experimental values. The 2NN MEAM potential shows slightly greater anharmonicity for temperatures higher than 500 K compared to experimental results.[6] Therefore, the 2NN MEAM potential gives a better description for both the harmonic and anharmonic properties of silicon.

III. THERMAL CONDUCTIVITY PREDICTION OF BULK SILICON RANGING FROM 500 TO 950 K

As mentioned in the previous section, among the five potentials chosen to be studied in this paper, 2NN MEAM, SW, and Tersoff III give comparable results on the basis of vibrational behavior. These potentials should therefore be suitable for thermal studies using MD simulations. In this section, the thermal conductivity of bulk silicon is presented with the three potentials, and compared with the bulk thermal conductivity for natural silicon, ranging from 500 to 950 K.[36] As the computational time required for the bulk thermal conductivity calculation is non-trivial, only the SW, Tersoff III, and 2NN MEAM potentials were used. The Tersoff II and 1NN MEAM potentials are not considered here because of their discrepancy between their prediction to the experimental dispersion curves and linear thermal expansion.

Several methods can be used to predict thermal conductivity using MD: equilibrium MD (EMD),[37–39] homogeneous non equilibrium MD (HNEMD),[40,41] and non homogeneous non equilibrium molecular dynamics (NHNEMD or NEMD). The latter is certainly the most widely used. NEMD can be implemented in two ways: by the imposed heat flux method[14,20–22] or the imposed temperature method.[23–25] The imposed temperature method consists of imposing a temperature gradient across a structure and then calculating the heat flux between the thermostated zones in steady state.

Periodic boundary conditions were applied to the system. A temperature gradient was created by imposing a hot

temperature in a volume positioned at the center of the system, and a cold temperature at the two ends of the system (in the z direction). This configuration allows us to respect the periodic boundary conditions. Thermal conductivity was calculated using Fourier's law. The method proposed by Lukes *et al.*[20] is used to calculate the uncertainty.

Nonlinear response effects should be negligible when considering Fourier's law. Schelling *et Al.*[22] showed that thermal conductivity does not depend strongly on the magnitude of heat added, in a thin slab, $\Delta\varepsilon/A$, at each MD time step, where $\Delta\varepsilon$ is the heat added and A is the system cross-section. For small values of $\Delta\varepsilon/A$, the temperature difference between the hot and cold ends of the simulation cell becomes comparable to typical statistical noise. For large values of $\Delta\varepsilon/A$, there were no significant deviations from Fourier's law. To take into account suitable values for $\Delta\varepsilon/A$, the difference imposed for the temperatures considered was 10% of the mean temperature value. This approach leads to $\Delta\varepsilon$/A values ranging from 1.4 to 4.8 x 10^{-4} eV/nm^2 for systems with dimensions 5×5 in the x and y directions. These values appeared to be suitable and in good agreement with the Schelling *et al.* values for systems of dimensions 4×4.

The phonon mean free path is much lower at high temperature than at ambient temperature. Thus, heat transfer simulations ranging from 500 to 950 K were carried out in systems of dimensions from 54.3 to 651.6 nm in the z direction. Consequently, the regime in which the size of the system is bigger than the phonon mean-free path could be considered.[22] In addition, Schelling *et al.*[22] showed that a strong nonlinear temperature profile can be observed within a few nanometers of the source or sink region, attributable to the strong scattering caused by either the heat source or heat sink. Halfway between the heat source and heat sink, the temperature profile was fitted with a linear function, and the resulting temperature gradient was used to obtain the thermal conductivity.

As the heat is mainly carried by acoustic modes, the equation for the thermal conductivity as a function of system length and phonon mean-free path is[22]

$$\frac{1}{\lambda} = \frac{\alpha_0^3}{4k_B \upsilon}\left(\frac{1}{l_\infty} + \frac{4}{L_z}\right), \quad (1)$$

where k_B is the Boltzmann constant, v is the group velocity of the acoustic branch, l_∞ is the mean-free path for an infinite system, and the length of the simulation cell is L_z. This equation gives an estimation of the slope of the $1/\lambda$ function of $1/L_z$ and allows extrapolating the value of the thermal conductivity for an infinite size system.

The thermal conductivity values for silicon at 500, 700, and 950 K obtained with the SW, Tersoff III and 2NN MEAM potentials, and the values obtained by Schelling *et al.*[22] using the SW potential are depicted in Fig. 4. These values are compared with experimental values for natural silicon ranging from 500 to 950 K (Ref. 36) and the predicted values of isotopically pure silicon by Kazan *et al.*[33]

The values obtained for the SW potential are in good agreement with the values from Schelling *et al.*[22] for thermal conductivity using NEMD with an imposed heat flux. Tersoff III and SW overestimate thermal conductivity of natural silicon by more than 50%, while the 2NN MEAM potential underestimates it by less than 30%. Therefore, the 2NN MEAM potential seems to give results closer to experimental values for thermal conductivity of natural silicon. However, the MD simulations do not take into account phonon scattering due to the presence of two main isotopes in natural silicon. MD should give rise to thermal conductivity values higher than the experimental ones. Kazan *et al.*[33] predicted thermal conductivity values for isotopically enriched silicon Fig. 4, which are closer than the results obtained with the Tersoff III potential. As a conclusion, even if the 2NN MEAM gives the best description for the harmonic and anharmonic silicon properties, it underestimates the thermal conductivity of natural silicon. On the other hand, the values obtained with the Tersoff III potential are in a better qualitative agreement with the experimental results either for natural or for isotopically enriched silicon. Thus, the choice of interatomic potential for MD simulation of heat transfer remains a non-trivial task. The difference between the thermal conductivities of natural and isotopically silicon suggests that MD simulations of heat transfer in natural silicon should take into account the mass difference. This has never actually been studied and was not within the scope of the current paper.

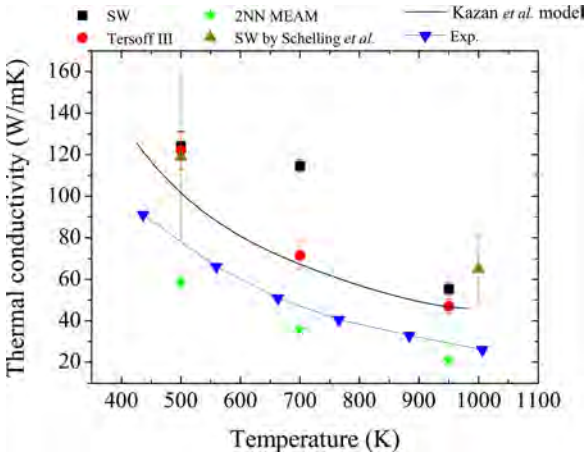

FIG. 4. (Color online) Thermal conductivity as a function of temperature for SW potential, Tersoff III, and 2NN MEAM at 500, 700, and 950 K. These values are compared to the experimental values (Ref. 36), the predicted values of isotopically pure silicon by Kazan *et al.* (Ref. 33), and the values obtained by Schelling *et al.* (Ref. 22) using the SW potential.

IV. THERMAL CONDUCTIVITY OF SI NANOWIRES

The choice of interatomic potential is a difficult issue and can lead to poor results if not made correctly. Moreover, Gomes *et al.*[27] showed that the choice of boundary conditions has a strong influence on the thermal conductivity of nanofilms. In this section, the influence of boundary conditions on the thermal conductivity of silicon (001) nanowires was studied for the five potentials under consideration in this paper. Nanowires were chosen instead of nanofilms for reasons of computational time.

The cross-section of nanowire has a square shape. The lateral surfaces of the nanowires are perpendicular to the

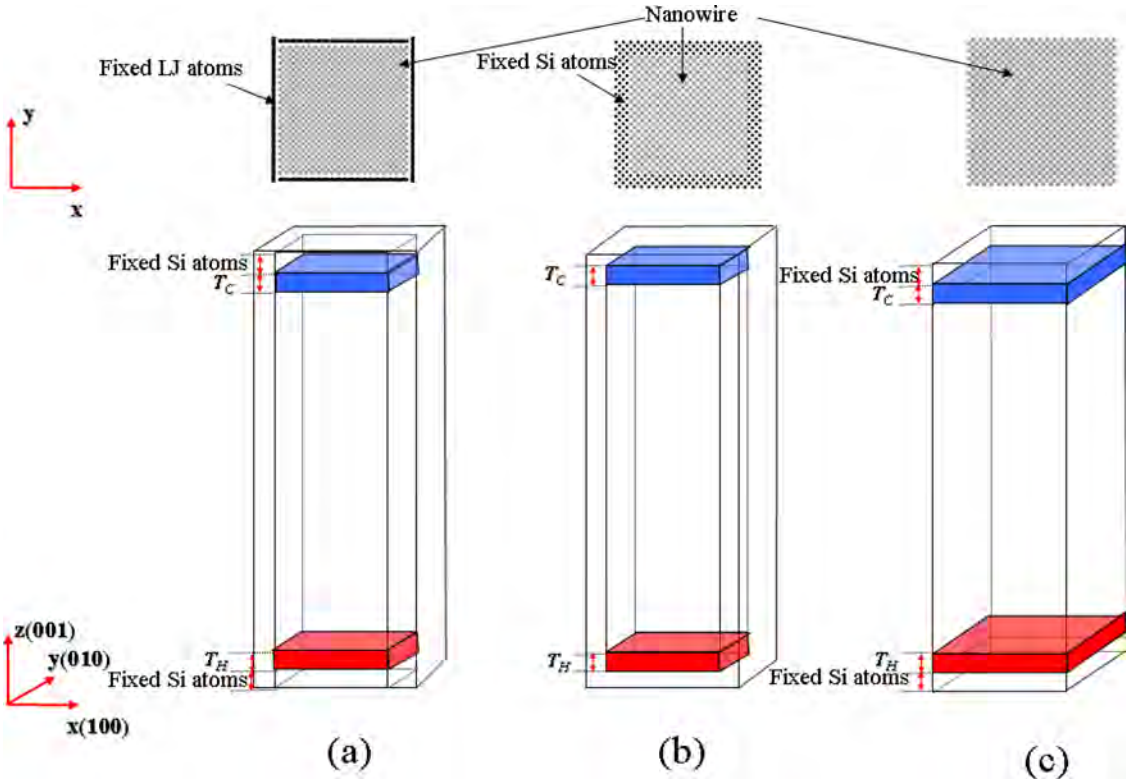

FIG. 5. (Color online)Cross-section configurations used to simulate the thermal conductivity of silicon nanowires. Configuration (a) potential wall, (b) fixed silicon atoms in all directions, and (c) free boundary conditions in x ((100) direction) and y ((010) direction) directions.

(100) and (010) directions that are parallel to the x and y directions of the reference frame. To avoid interaction between nanowire surfaces, the box size in the x and y directions is larger than the system size. This is equivalent to using free boundary conditions. However, if no other constraints are added to the system, unexpected and undesirable phenomena may occur, such as nanowire twisting, sublimation,[27] etc. Certain solutions can be used to avoid these phenomena, for example, potential walls and fixed atoms (Fig. 5). Heat transfer is simulated by hot and cold reservoirs placed at the ends of the nanowire (Fig. 5), while a layer of fixed atoms above and below the thermostated zones is used to avoid nanowire deformation. For the first configuration (Fig. 5(a)), potential walls are added around the nanowire surfaces that are parallel to the z direction.[42] These walls are created by placing fixed atoms at a distance d from the silicon nanowire and a Lennard Jones potential interaction between these fixed atoms and the silicon atoms. The distance d between the surface atoms in x ((100) direction) and y ((010) direction) planes is 2.64 Å. In the second configuration, the nanowire is surrounded by fixed silicon atoms (Fig. 5(b)). In the third configuration, there is no other constraint than the fixed silicon atoms added above and below the top and the bottom heat sources to stabilize the nanowire (Fig. 5(c)).

Thermal conductivity is extracted from the calculation of the temperature and the heat flux crossing the nanowire between the two sources, as described in the previous section. In our simulations, the average temperature of the nanowires is 300 K and the temperature difference between hot and cold zone is equal to 30 K. The thickness of the two reservoirs for all three methods was kept constant and equal to 2 monolayers. The time step was 0.5 fs.

The number of time steps required for the statistics, (N_e) and to reach the steady state, (N_s), depends on system size, configuration, and interatomic potentials. Table I gives the values for N_s and N_e used on the smallest and largest nanowires. The Tersoff III potential requires much more computational time for configurations (a) and (c) than the other potential.

The linearity of the temperature profile is an indication of the diffusive regime. In this regime, there is no strong scattering due to hot and cold sources. A linear temperature profile was observed for the structures studied. The linearity of the temperature profile is due to the decrease of the phonon mean free path value for silicon nanostructures, already verified in previous results in the literature.[28,42,43] Therefore, the diffusive regime can be considered and Fourier's law applied.

TABLE I. Number of time steps required to reach the steady state (N_s) and for the statistics (N_e) for the smallest (2.17 nm of cross-section width and 10.86 nm of length) and the largest (4.34 nm of cross-section width and length of 27.15 nm) used to simulate heat transfer.

	All potentials and configs. except for Tersoff III (configs. (a) and (c))		Tersoff III (Config. (a) and (c))	
	(N_s)	(N_e)	(N_s)	(N_e)
Smallest	150 000	1 million	300 000	2 million
Largest	1 million	5 million	2.5 million	8 million

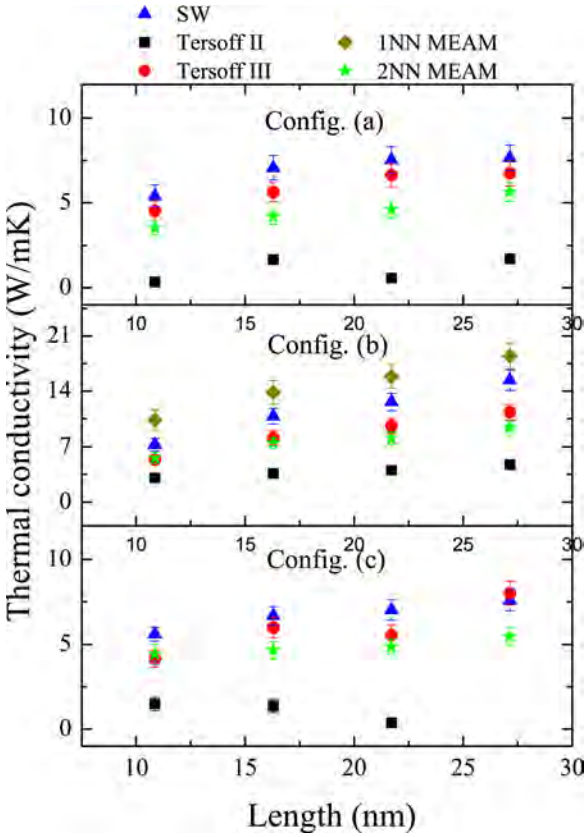

FIG. 6. (Color online)Thermal conductivity as a function of nanowire length for different potentials and different configurations at a mean temperature of 300 K and cross-section of 4.34 nm.

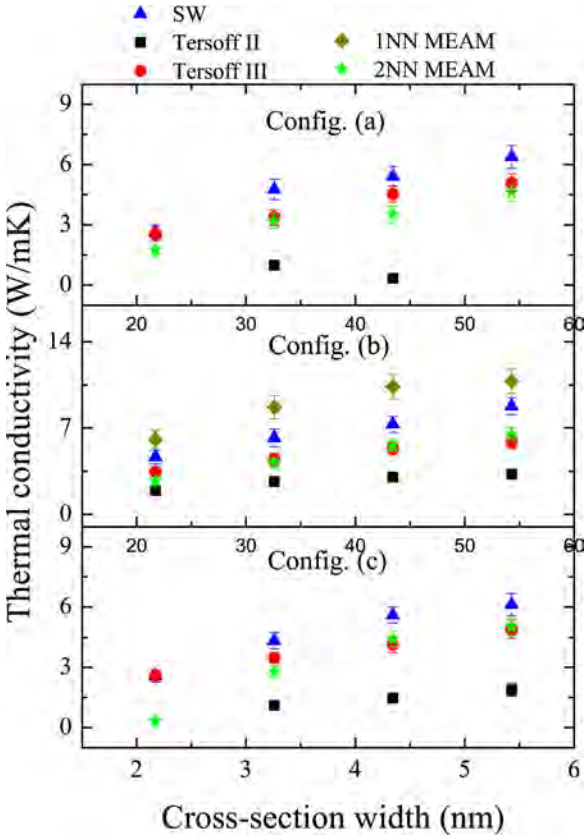

FIG. 7. (Color online)Thermal conductivity as a function of cross-section width for different potentials and different configurations at a mean temperature of 300 K and a fixed length of 11 nm.

To study the influence of nanowire length on thermal conductivity, the nanowires were given lengths from 11 to 27 nm, and cross-section of 4.34 nm (8×8 lattice parameters). The thermal conductivities obtained for the five potentials and the three configurations are shown in Fig. 6. The influence of the nanowire's cross-sectional width on thermal conductivity was also studied for the five potentials and three configurations. For this study, the nanowires were given fixed length of 11 nm, and a cross-sectional width ranging from 2.2 to 5.4 nm.[7] Results are missing for 1NN MEAM and Tersoff II potentials. Configurations (a) and (c) were not stable when using 1NN MEAM potential for all systems, and stability was system size dependent when using Tersoff II. In these cases, the time step was decreased at least by a factor of ten in order to attempt to avoid instabilities without success. This phenomenon is well known[43] and solutions were proposed, which consists of relaxing the system using configuration (b), and then following the simulations with configurations (a) and (c) However, it is not used here as the aim was to test the ability of each potential for a given simulation strategy.

Thermal conductivity increases as length and cross-sectional width increase, and thermal conductivity is more than two orders of magnitude lower than the bulk value. The Tersoff II potential underestimates the acoustic and longitudinal modes for the bulk dispersion curves and has a non-physical negative thermal expansion coefficient. This explains why this potential gives the lowest values of the thermal conductivity and wrong tendencies. The 1NN MEAM potential reproduces correct tendencies thanks to its positive thermal expansion coefficient, but, as it considerably overestimates the bulk dispersion curves, it gives the highest thermal conductivity values. Configuration (b) leads to results twice as high as the thermal conductivity prediction made for the two other configurations, which are also greater than the experimental value. Gomes *et al.*[27] studied the influence of these configurations on the atomic vibrations by using the SW potential for thin films. Similar in-plane thermal conductivities were predicted by using the three configurations, except for small thicknesses (smaller than 10 nm). This is in good agreement with the results obtained with SW, Tersoff III, and 2NN MEAM potentials for configurations (a) and (c). For configuration (b), when the nanowire is limited by a layer of frozen atoms, thermal conductivity increases as the vibrational amplitude of the atoms located near the frozen ones decreases. Configuration (c) is considered to be the most similar to the hot-plate experiment setup. As thermal conductivity values are similar for configurations (a) and (c) both of them can be considered equivalents for determining thermal conductivity.

The results are difficult to compare with experimental results since the smallest nanowire that has been experimentally characterized has a cross-section diameter of 22 nm, five times larger than the maximum nanowire cross-section used in our MD simulations.[44] Moreover, the simulated nanowires are perfect, without surface oxide or surface roughness, thus overestimating thermal conductivity for a real nanowire. The predicted values values are higher than the results from Wang

et al. using the NEMD,[42] because they made a quantum correction for nanowire temperatures. Compared to previous theoretical[42,43] and experimental[44] results for Si nanowire thermal conductivity, our results, except for the Tersoff II potential, exhibit the same tendencies: thermal conductivity increases as the length and the cross-section increase. For an equivalent Si nanowire of 2.17 nm cross sectional width and a length of 10.86 nm, our value obtained using the SW potential (2.7 W/mK) is higher than the one obtained previously by Volz and Chen[43] of 1.35 W/mK (see Fig. 7). This difference is explained since Volz and Chen used EMD, which is known to give smaller values then NEMD.[45,46]

V. CONCLUSIONS

Five interatomic potentials were evaluated for MD heat transfer simulations in Si: SW, Tersoff II and III, 1NN MEAM, and 2NN MEAM. The 2NN MEAM potential is in better agreement with experimental values of the dispersion curves and linear thermal expansion than the Tersoff III and SW potentials. The Tersoff II potential gives a negative linear thermal expansion, and it strongly underestimates the dispersion curves. The 1NN MEAM potential for silicon strongly overestimates dispersion curves as well. These two latter potentials should not be used for heat transfer MD simulations. Among the five potentials considered here, the 2NN MEAM potential gives the best results compared to experimental data for the thermal conductivity of bulk natural silicon. However, the MD simulation results should be compared with thermal conductivity of isotopically pure silicon since the mass difference of the isotopes in natural silicon is not taken into account. In these conditions, it appears that the Tersoff III potential is the most appropriate, even if its descriptions of vibrational properties are not as good as those given by the 2NN MEAM potential.

Central processing unit time (CPU) depends on the potential and on boundary conditions. For the Tersoff III potential, configurations (a) and (c) considerably increase the simulation time of nanowires. In addition, the Tersoff II, Tersoff III, 1NN MEAM, and 2NN MEAM potentials lead to greater simulation times than the SW potential. For the Tersoff III and the 2NN MEAM potentials, CPU times are 60% and 90% greater than the times for SW potential using configuration (b). For the Tersoff III potential and configurations (a) and (c), the simulations times are greater than 200% than SW potential.

With exception of Tersoff II, the thermal conductivities predicted here for silicon nanowires are in good agreement with previous experimental[47] and theoretical results.[42,43] The correct order of magnitude is obtained, and as expected the thermal conductivity increases when increasing the cross-section and the length of nanowires. For the MEAM potential, the results show that considering the interactions between the second nearest neighbors (the 2NN MEAM potential) considerably improves the potential for heat transfer simulations. It allows using boundary conditions under which the 1NN MEAM potential demonstrates instability. The influence of boundary conditions on the thermal conductivity is also studied. Two of them (configurations (a) and (c)) give comparable results although configuration (c) is actually the more realistic one. Configuration (b), which consists of a fixed layer of silicon atoms all around the nanowire, leads to results twice as high as for configurations (a) and (c), confirming previous conclusions obtained for nanofilms.

ACKNOWLEDGMENTS

This work was funded by the CNRS in the framework of the ANR-New researchers NanoMetrETher and ANR COFISIS projects, ANR-07-NANO-047-03. The authors are grateful for the use of the large computer facilities; CNRS-IDRIS and the P2CHPD of the FLCHP (Fédération Lyonnaise de Calcul Haute Performance).

[1]M. L. Green, P. K. Schenck, K.-S. Chang, J. Ruglovsky, and M. Vaudin, Mic. Eng. **86**, 1662 (2009).
[2]G. Vastola, A. Marzegalli, F. Montalenti, and L. Miglio, Mat. Sci. Eng. B **159-60**, 90 (2009).
[3]M. Liu, Y. Lu, J. Zhang, S. Xia, and J. Yang, Microel. Eng. **86**, 2279 (2009).
[4]K.-N. Lee, D.-S. Lee, S.-W. Jung, Y.-H. Jang, Y.-K. Kim, and W.-K. Seong, J. Micromech. Microeng. **19**, 115011 (2009).
[5]M. Z. Bazant, E. Kaxiras, and J. F. Justo, Phys. Rev. B **56**, 8542 (1997).
[6]B.-J. Lee, Comp. Coup. P. Diag. Therm. **31**, 95 (2007).
[7]S. J. Cook and P. Clancy, Phys. Rev. B **47**, 7686 (1993).
[8]S. L. Prince, Comput. Simul. Mater. Sci. **205**, 183 (1991).
[9]K. Nordlund and S. L. Dudarev, C. R. Phys. **9**, 343 (2008).
[10]F. H. Stillinger and T. A. Weber, Phys. Rev. B **31**, 5262 (1985).
[11]J. Tersoff, Phys. Rev. Lett. **56**, 632 (1986).
[12]J. Tersoff, Phys. Rev. B **37**, 6991 (1988).
[13]J. Tersoff, Phys. Rev. B **38**, 9902 (1988).
[14]J. F. Justo, M. Z. Bazant, E. Kaxiras, V. V. Bulatov, and S. Yip, Phys. Rev. B **58**, 2539 (1998).
[15]T. J. Lenosky, B. Sadigh, E. Alonso, V. V. Bulatov, T. D. Rubia, J. Kim, A. F. Voter, and J. D. Kress, Modelling Simul. Mater. Sci. Eng. **8**, 825 (2000).
[16]B. Bolding and H. C. Andersen, Phys. Rev. B **41**, 10568 (1990).
[17]M. I. Baskes, J. S. Nelson, and A. F. Wright, Phys. Rev. B **40**, 6085 (1989).
[18]M. I. Baskes, Phys. Rev. B **46**, 2727 (1992).
[19]B.-J. Lee and M. I. Baskes, Phys. Rev. B **62**, 8564 (2000).
[20]J. R. Lukes, D. Y. Li, X.-G. Liang, and C.-Tien, J. Heat Transfer **122**, 536 (2000).
[21]T. Ikeshoji and B. Hafskjold, Mol. Phys. **81**, 251 (1994).
[22]P. K. Schelling, S. R. Phillpot, and P. Keblinski, Phys. Rev. B **65**, 144306 (2002).
[23]B. C. Daly and H. J. Maris, Physica B **316-317**, 247 (2002).
[24]J. L. Barrat and F. Chiaruttini, Mol. Phys. **101**, 1605 (2003).
[25]K. Termentzidis, P. Chantrenne, and P. Keblinski, Phys. Rev. B **79**, 214307 (2009).
[26]S. Plimpton, J. Comput. Phys. **117**, 1 (1995).
[27]C. J. Gomes, M. Madrid, J. V. Goicochea, and C. H. Amon, J. Heat Transfer **128**, 1114 (2006).
[28]P. Heino, Eur. Phys. J. B **60**, 171 (2007).
[29]L. J. Porter, J. F. Fausto, and S. Yip, J. Appl. Phys. **82**, 5378 (1997).
[30]N. I. Papanicolaou, I. E. Lagaris, and G. A. Evangelakis, Surf. Sci. **337**, L819 (1995).
[31]C. Flensburg and R. F. Stewart, Phys. Rev. B **60**, 284 (1999).
[32]P. Chantrenne, J. L. Barrat, X. Blase, and J. D. Gale, J. Appl. Phys. **97**, 104318 (2005).
[33]M. Kazan, G. Guisbiers, S. Pereira, M. R. Correia, P. Masri, and A. Bruyant, J. Appl. Phys. **107**, 083503 (2010).
[34]S. Ryu, C. R. Weinberger, M. I. Baskes, and W. Cai, Modelling Simul. Mater. Sci. Eng. **17**, 075008 (2009).
[35]D. A. Broido, A. Ward, and N. Mingo, Phys. Rev. B **72**, 014308 (2005).
[36]C. Mion, J. F. Muth, E. A. Preble, and D. Hanser, Appl. Phys. Lett. **89**, 092123 (2006).
[37]D. Frenkel and S. Berend, *Understanding Molecular Dynamics Simulation* (Academic, San Diego, 1996).

[38]M. P. Allen and D. J. Tildesley, *Computer Simulation of Liquids* (Oxford University Press, New York, 1997).
[39]R. Zwanzig, Ann. Rev. Phys. Chem. **16**, 67 (1964).
[40]D. J. Evans, J. Chem. Phys. **78**, 3297 (1983).
[41]D. J. Evans, W. G. Hoover, B. H. Failor, B. Moran, and A. J. C. Ladd, Phys. Rev. A **28**, 1016 (1983).
[42]S.-C. Wang, X.-G. Liang, X.-H. Xu, and T. Ohara, J. Appl. Phys. **105**, 014316 (2009).
[43]S. G. Volz and G. Chen, App. Phys. Lett. **75**, 2056 (1999).
[44]D. Li, Y. Wu, P. Kim, L. Shi, P. Yang, and A. Majumdar, Appl. Phys. Lett. **83**, 2934 (2003).
[45]K. Termentzidis, S. Merabia, P. Chantrenne, and P. Keblinski, Int. J. Heat Mass Transf. **22**, 475001 (2010).
[46]E. Landry, M. Hussein, and McGauchey, Phys. Rev. B **77**, 184302 (2008).
[47]J.-H. S. B.-J. Lee and M. I. Baskes, Phys. Rev. B **68**, 144112 (2003).